Particle coagulation and the memory of initial conditions

1998 J. Phys. A: Math. Gen. 31 9241

(http://iopscience.iop.org/0305-4470/31/46/014)

J. Phys. A: Math. Gen. **31** (1998) 9241–9254. Printed in the UK PII: S0305-4470(98)95888-7

Particle coagulation and the memory of initial conditions

Alexandria B Boehm†, Cris Poor‡ and Stanley B Grant†§

† Department of Civil and Environmental Engineering, University of California, Irvine, CA 92697, USA

‡ Department of Mathematics, Fordham University, Bronx, New York 10458, USA

Received 14 July 1998

Abstract. Particle coagulation is mathematically described by an infinite set of coupled nonlinear differential equations. A solution to these equations is derived for the case in which all particle clusters possess the same reactivity (i.e. a constant kernel) and where the initial conditions are bimodal, consisting of monomers and any sized J-mers. Properties of the solution are explored and it is shown that the scaling theory developed by Swift and Friedlander (1964 *J. Colloid. Sci.* **19** 621) and extended by van Dongen and Ernst (1984 *Phys. Rev. Lett.* **54** 1396) applies to all cluster sizes only in the limit $t \to \infty$, as reported previously by Kreer and Penrose (1994 *J. Stat. Phys.* **75** 389). At finite times we find distinctly different scaling properties for the small and large ends of the size spectrum. Furthermore, at all times the shape of the small end of the size spectrum retains a memory of the initial conditions. These results may apply to other modes of coagulation so long as interactions between small clusters, and between small and large clusters, are as weak as the constant kernel employed here.

1. Introduction

The kinetic equation describing the time evolution of small particles undergoing irreversible coagulation in a homogeneous medium was formulated by von Smoluchowski (1917) at the beginning of this century:

$$\frac{\mathrm{d}n_j(t)}{\mathrm{d}t} = \sum_{i=1}^{j-1} K_{i,j-i} n_i n_{j-i} - 2\sum_{i=1}^{\infty} K_{i,j} n_i n_j. \tag{1}$$

Here n_j is the number concentration of clusters containing j primary particles (or 'j-mers'), and $K_{i,j}$ is a rate constant that describes coagulation between an i-mer and a j-mer. The r.h.s. of this equation models the rate at which j-mers are formed by the binary clustering of i-mers and $(j-i)$-mers (first term), and the rate at which j-mers are lost to coagulation with all other cluster sizes (second term). Application of (1) to the study of particle coagulation is complicated by the mathematical difficulties associated with solving the governing equation (Hidy 1965, Hidy and Lilly 1965, Kobraei and Duncan 1986, Erasmus *et al* 1994, Eyre 1995) and our limited understanding of the physical and surface-chemical processes that govern the mathematical form of the rate matrix or 'kernel', $K_{i,j}$. To date, familiar solutions to (1) have been found only for a few algebraically simple forms of the kernel, including the constant kernel ($K_{i,j} = K_{1,1}$), the sum kernel ($K_{i,j} = K_{1,1}(i + j)/2$), the product kernel ($K_{i,j} = K_{1,1}ij$) and linear combinations of these (von Smoluchowski 1917, Melzak 1953,

§ Author to whom correspondence should be addressed. E-mail address: sbgrant@uci.edu

0305-4470/98/469241+14$19.50

McLeod 1962, Spouge 1983, Bak and Lu 1987, Binglin 1987, Gabellini and Meunier 1992, Treat 1992).

It has been postulated that the cluster-size distributions predicted by (1) are self-similar, in that they collapse onto a single curve when properly scaled. This self-similar feature of the cluster-size distribution implies that it can be written in the following factored form as $t \to \infty$ with $j/s(t)$ fixed:

$$n_j(t) \sim s(t)^{-2}\psi(j/s(t)). \tag{2}$$

The function $s(t)$ is some measure of the average cluster size and $\psi(\eta)$ represents the shape of the cluster-size distribution (Friedlander and Wang 1966, van Dongen and Ernst 1984, Gabellini and Meunier 1992). In this analysis, it is assumed that $\psi(\eta)$ is 'universal', whereby we mean that it does not depend on the initial conditions. As proposed by van Dongen and Ernst (1984), hereafter referred to as VDE, the nature of the functions $s(t)$ and $\psi(\eta)$ depends on two mathematical features of the kernel: the homogeneity, λ, of $K_{i,j}$ with respect to its arguments i and j, and the exponent μ that governs the small i/j limit of $K_{i,j}$. The magnitude and sign of λ determines whether the reactivity between clusters of the same size grows ($\lambda > 0$) or decreases ($\lambda < 0$) with cluster size, while μ determines whether clustering occurs preferentially between clusters of the same size ($\mu > 0$) or between clusters of vastly different size ($\mu < 0$). The predicted relationships between the mathematical features of the kernel (i.e. μ and λ) and the resultant cluster-size distribution (i.e. $s(t)$ and $\psi(\eta)$) are presented elsewhere (van Dongen and Ernst 1984, Broide and Cohen 1992, Gabellini and Meunier 1992).

Validation of the above similarity theory has come from experimental investigations (Swift and Friedlander 1964, Friedlander and Wang 1966, Weitz *et al* 1984, Bolle *et al* 1987, Matsoukas and Friedlander 1991, Broide and Cohen 1992, Olivier *et al* 1992, Fernández-Barbero *et al* 1996, Mishra *et al* 1998), computer simulations of the clustering process (Jullien *et al* 1984, Vicsek and Family 1984, Meakin *et al* 1985, Meakin 1987), and detailed analyses of the solutions to (1) (Mulholland *et al* 1977, Jullien 1990, Gabellini and Meunier 1992, Kreer and Penrose 1994). Of the solutions, the constant kernel solution has received considerable attention because it closely approximates the physical system where coagulation is rate-limited by how fast clusters can diffuse into contact (Broide and Cohen 1992, Fernández-Barbero *et al* 1996): so-called diffusion-limited cluster–cluster aggregation (DLA). Provided that there are no clusters initially present, von Smoluchowski (1917) showed that the solution to (1) for the choice of a constant kernel is given as follows:

$$n_j(t) = N_\infty(0)\frac{(t/t_c)^{j-1}}{(1+t/t_c)^{j+1}} \tag{3}$$

where $N_\infty(0)$ is the zeroth moment of the size distribution at $t = 0$. The parameter $t_c = 1/(K_{1,1}N_\infty(0))$ represents the characteristic timescale for the formation of dimers by coagulation of single particles. Relative to the VDE similarity predictions presented earlier, it is easy to show that in the limit of long-time, n_j develops the self-similar form predicted by (2) with $\psi(\eta) = \mathrm{e}^{-\eta}$ and $s(t) \sim t$ (Swift and Friedlander 1964). Experimental measurements of particle-size distributions undergoing DLA reveal that the average cluster-size $s(t)$ increases linearly with time as predicted, but that the cluster-size distribution $\psi(\eta)$ does not decline monotonically with η. The latter disagreement between theory and experiment has been attributed to the fact that the constant kernel fails to account for the preferential scavenging of small clusters by large clusters characteristic of DLA (Broide and Cohen 1992, Fernández-Barbero *et al* 1996).

Von Smoluchowski's solution to (1) for the constant kernel is valid for monodisperse initial conditions. However, there are many examples of physical systems where the particles

are initially distributed between two or more cluster sizes (i.e. polydisperse). Mulholland *et al* (1977) investigated the influence of broad and narrow initial size distributions on the scaling properties of the large end of the size spectrum. These researchers found that the self-similar nature of the large end of the size spectrum was not independent of the initial conditions, or universal, when the initial size distribution was broad. The focus of this study is to investigate to what extent the memory of initial conditions is preserved in the small end of the size spectrum. We accomplish this by solving (1) with a constant kernel and a bimodal initial distribution consisting of monomers and any size J-mers.

The paper is organized as follows. We derive this new solution in section 2 and present illustrative examples of the predicted cluster-size distribution in section 3. In section 4, we investigate limitations of the scaling form given by (2) and present a new scaling relationship for the small end of the size spectrum.

2. Derivation of solution

We begin by recasting (1) into a non-dimensional form:

$$\frac{\mathrm{d}\bar{n}_j(\tau)}{\mathrm{d}\tau} = \sum_{i=1}^{j-1} \bar{n}_i \bar{n}_{j-i} - 2\bar{n}_j \sum_{i=1}^{\infty} \bar{n}_i \tag{4}$$

where $\bar{n}_j = n_j / N_\infty(0)$ is the reduced form of the fluid concentration of j-mers, $\tau = t/t_c$ is reduced time, and $N_\infty(0)$ is the total number concentration of clusters at $\tau = 0$. Equation (4) may be further simplified by recalling the definition of the zeroth moment, $\bar{N}_\infty = \sum_{j=1}^{\infty} \bar{n}_j$ and defining $\bar{n}_0(\tau) \equiv -\bar{N}_\infty(\tau)$:

$$\frac{\mathrm{d}\bar{n}_j(\tau)}{\mathrm{d}\tau} = \sum_{i=0}^{j} \bar{n}_i \bar{n}_{j-i}. \tag{5}$$

We introduce a generating function

$$g(x, \tau) \equiv \sum_{j=0}^{\infty} \bar{n}_j(\tau) x^j \tag{6}$$

for which a partial differential equation is developed by differentiating with respect to τ, and substituting (5):

$$\partial_\tau g(x, \tau) = g(x, \tau)^2. \tag{7}$$

This is a Bernoulli differential equation for which a solution may be found by changing the dependent variable to $g(x, \tau)^{-1}$:

$$g(x, \tau) = 1/[-\tau + 1/g(x, 0)]. \tag{8}$$

Here $g(x, 0)$ is the generating function that describes the initial condition, and thus the cluster-size distribution, at $\tau = 0$.

We wish to solve (1) subject to the following initial conditions:

$$\bar{n}_1(0) = \alpha \tag{9a}$$

$$\bar{n}_J(0) = \beta \tag{9b}$$

$$\bar{n}_j(0) = 0 \qquad j \neq 1, J \tag{9c}$$

where $\alpha, \beta > 0$ and $\alpha + \beta = 1$. This represents a bimodal distribution where the fraction of the total particle concentration initially distributed between monomers and J-mers is given by α and β, respectively.

Given these initial conditions for $\bar{n}_j(0)$, $g(x,0)$ has the form

$$g(x,0) = -1 + \alpha x + \beta x^J \tag{10}$$

and (8) becomes

$$g(x,\tau) = \frac{-1 + \alpha x + \beta x^J}{(1+\tau) - \tau(\alpha x + \beta x^J)}. \tag{11}$$

In order to develop an expression for $\bar{n}_j(\tau)$, the generating function is expressed in increasing powers of x. The final result is

$$\bar{n}_j(\tau) = \frac{1}{(1+\tau)^2} \sum_{l=0}^{\frac{j}{J-1}} \binom{j - l(J-1)}{l} \alpha^{j-lJ} \beta^l \left(\frac{\tau}{1+\tau}\right)^{j-1-l(J-1)} \tag{12}$$

where

$$\binom{a}{b} = \frac{a!}{(a-b)!b!}.$$

The algebraic manipulations involved in the last step are presented in the appendix. A recurrence relation is also available for solutions to (4), where $j \geqslant J$:

$$(1 + 1/\tau)\bar{n}_{j+1}(\tau) = \alpha \bar{n}_j(\tau) + \beta \bar{n}_{j+1-J}(\tau). \tag{13}$$

Equation (13) is a direct consequence of the expression for the generating function given in (11).

3. Illustrative examples of predicted cluster-size distribution

In this section we examine the influence of the parameters α, β and J on the cluster-size distribution predicted by our solution. In figure 1, the cluster-size distribution, $\bar{n}_j$, is plotted against j for the case where equal number concentrations of monomers and 4-mers are allowed to coagulate for a total of 10 coagulation timescales (i.e. $\alpha = \beta = 0.5$, $J = 4$ and $\tau = 10$). The pattern observed here is typical for all cluster-size distributions with $J > 1$: the distribution is oscillatory for small j and decays exponentially as $n_j \sim \exp(-jN_\infty(\tau)/N_1)$ for large j.

For the constant kernel used in our study, $\lambda = \mu = 0$ and, therefore, the reactivity between any two clusters is the same regardless of cluster size. The only factors affecting the rate at which clusters appear and disappear from the system are the number concentrations of clusters involved in the reactions. For this reason, we find peaks and holes in the cluster-size distribution resulting from any initially bimodal distribution. For the cluster distribution illustrated in figure 1, clustering between monomers and 4-mers generates peaks at $j = 1, 4, 9, 13, \ldots$ and holes at $j = 3, 7, 11, 16, \ldots$. The influence of time on the size distribution is illustrated in figure 2 for $J = 4, \alpha = \beta = 0.5$, and three different choices of τ. Oscillatory behaviour can be observed at the small end of the size spectrum even for $\tau = 100$. Hence, the small end of the size spectrum retains a memory of the initial condition even after the system has been coagulating for a very long time.

In figure 3, the cluster-size distributions are shown for several choices of α and β. All distributions correspond to $J = 4$ and $\tau = 10$. As the initial condition becomes dominated by monomers ($\alpha \to 1$), the peaks found at the small end of the size spectrum are increasingly less pronounced, and the cluster-size distribution approaches the exponential curve (full curve) characteristic of monodisperse initial conditions. This is a result of the ease with which all clusters are created when there is an abundance of monomers. As α

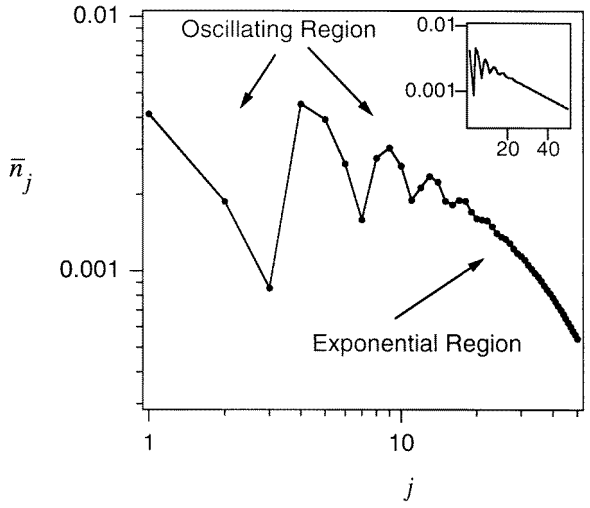

Figure 1. The typical shape of a cluster-size distribution resulting from a bimodal initial condition. Here the reduced cluster concentration, $\bar{n}_j$, is plotted for each cluster size, j. This particular cluster-size distribution is for initial conditions specified by $J = 4$ and $\alpha = \beta = 0.5$ at $\tau = 10$. A log–linear version of the same graph appears in the upper right-hand corner.

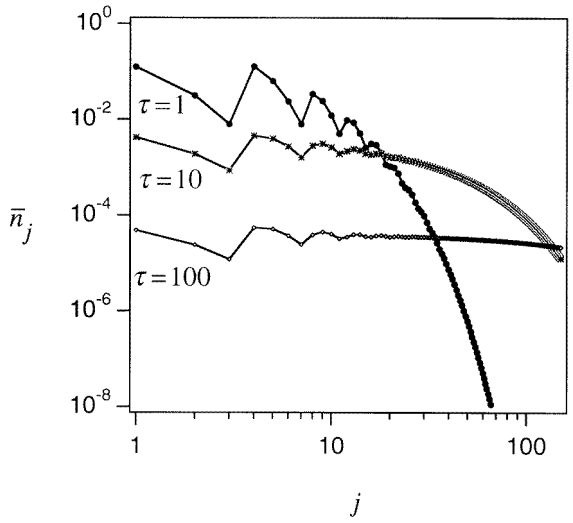

Figure 2. The time evolution of the cluster-size distribution resulting from initial conditions specified by $J = 4$ and $\alpha = \beta = 0.5$.

becomes smaller, the oscillatory behaviour of the small end of the spectrum becomes more pronounced and the oscillations extend farther into j-space.

The magnitude of J affects the shape of the cluster-size distribution by altering the distribution of particles between peaks and holes, and shifting the position of peaks and holes in j-space. Figure 4 shows the cluster-size distribution for $J = 1, 2$ and 4 when $\tau = 10$ and $\alpha = \beta = 0.5$. When $J = 2$, the distribution approaches the one that evolves from only monomers (full curve) because it is relatively easy to create all j-mers from

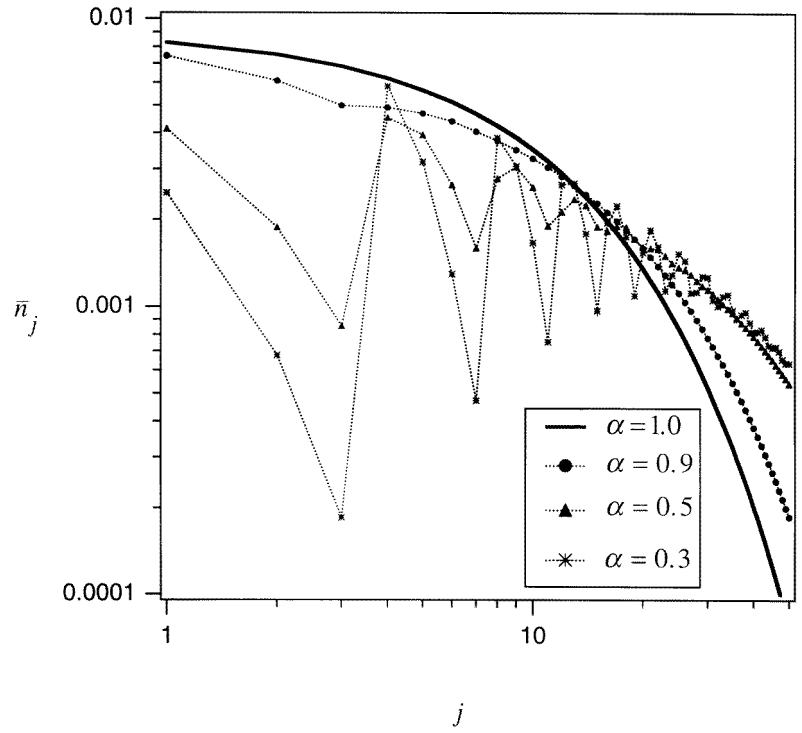

Figure 3. The effect of changing the initial distribution of particles between monomers (α) and J-mers (β) on the cluster-size distribution. Since $\beta = 1 - \alpha$, the distributions are labelled by their α-values only. All cluster-size distributions are for $\tau = 10$ and result from coagulation between a monomer and a 4-mer (i.e. $J = 4$).

monomers and dimers. When J becomes larger, peaks and holes extend farther into the size spectrum and the magnitude of the peaks and holes is more pronounced.

The transition from the oscillatory region to the exponentially decaying region, and the locations of the peaks and holes in the cluster-size distributions, can be rationalized as follows. We can express $\bar{n}_j(\tau)$ as a sum of oscillatory terms:

$$\bar{n}_j(\tau) = \frac{1}{\tau^2} \sum_{r_\tau} \frac{1}{g'(r_\tau)} \frac{1}{r_\tau^{j+1}} \tag{14}$$

where the sum is over the roots $z = r_\tau$ of $g(z) = g(z, 0) = 1/\tau$, (written here as if they were simple roots). This representation follows directly from the Cauchy residue formula and the complex integral:

$$\bar{n}_j(\tau) = \frac{1}{2\pi \mathrm{i}} \oint_{|z|=\varepsilon>0} g(z, \tau) \frac{\mathrm{d}z}{z^{j+1}} = \frac{1}{2\pi \mathrm{i}} \oint_{|z|=\varepsilon>0} \frac{g(z)}{1 - \tau g(z)} \frac{\mathrm{d}z}{z^{j+1}}. \tag{15}$$

For reasonably large τ, the roots r_τ of $g(z) = 1/\tau$ will be close to the roots of $g(z) = 0$. In the example above where $J = 4$ and $\alpha = \beta = 0.05$ we have

$$g(z) = \tfrac{1}{2}z^4 + \tfrac{1}{2}z - 1. \tag{16}$$

The four complex roots of (16) are $r_1 = 1$, $r_2 = -1.3532$, $w = 0.1766 + 1.2028\mathrm{i}$, and $\bar{w} = 0.1766 - 1.2028\mathrm{i}$. These roots will in general lie outside the unit circle and the modulus of the root $|r_\tau| > 1$ nearest to 1 will dominate the sum in (14) and govern the exponential

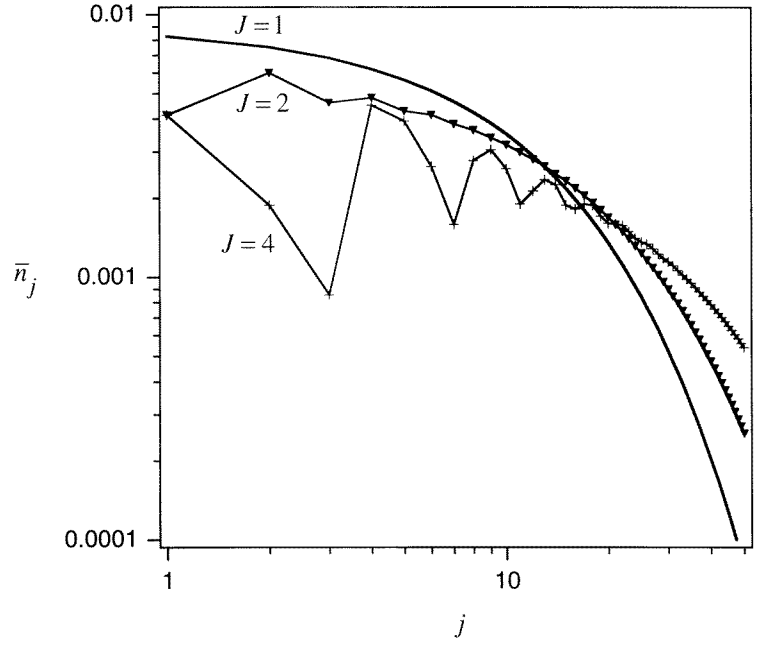

Figure 4. The effect of the cluster size, J, initially present with the monomer, on the cluster-size distribution. The distributions for $\tau = 10$, $\alpha = \beta = 0.5$ and $J = 1, 2$ and 4 are shown.

decay of $\bar{n}_j(\tau)$ as j increases. The closer the other roots, r_τ, are to the unit circle, the longer the oscillatory region will endure. In our example, the roots closest to the unit circle are w and $\bar{w}$ with $|w| = |\bar{w}| = 1.2157$; if we desire the leading term in (14) to dominate to N orders of magnitude then we want $\left|\frac{1}{w^{j+1}}\right| \sim 10^{-N}$ or $j + 1 \sim \frac{\ln(10)N}{\ln|w|}$. If $N = 2$, then $j \cong 22.5$. This explains the transition from the oscillatory region to the exponential decay region at approximately $j = 23$ in figure 1.

The locations of the peaks and holes in the cluster-size distributions may be explained using (14) as well. The peaks occur when the oscillatory terms $\frac{1}{g'(r_\tau)}\frac{1}{r_\tau^{j+1}}$ are in near conjunction with the positive real axis and the holes occur when these terms conjoin near the negative real axis. In the same example used above where $J = 4$ and $\alpha = \beta = 0.5$, for $j = 7$, the argument of the complex number $\frac{1}{g'(w)}\frac{1}{w^{j+1}}$ is about 174° so this gives a hole. For $j = 9$, the argument of $\frac{1}{g'(w)}\frac{1}{w^{j+1}}$ is about 11° and this gives a peak.

Finally, (14) can be used to investigate if the oscillatory behaviour of the small end of the size spectrum is unique to a bimodal initial distribution, or if it occurs for other polydisperse initial distributions as well. Figure 5 illustrates the location of the roots, r_τ, and the predicted cluster-size distributions resulting from the coagulation of a trimodal distribution (consisting of equal number concentrations of monomers, 4-mers and 8-mers) and a tetramodal distribution (consisting of equal number concentrations of monomers, 4-mers, 8-mers and 12-mers) at $\tau = 100$. As with the bimodal distributions described above, the two distributions illustrated in figure 5 exhibit oscillatory behaviour for small j, even after the systems have been coagulating for a long period of time.

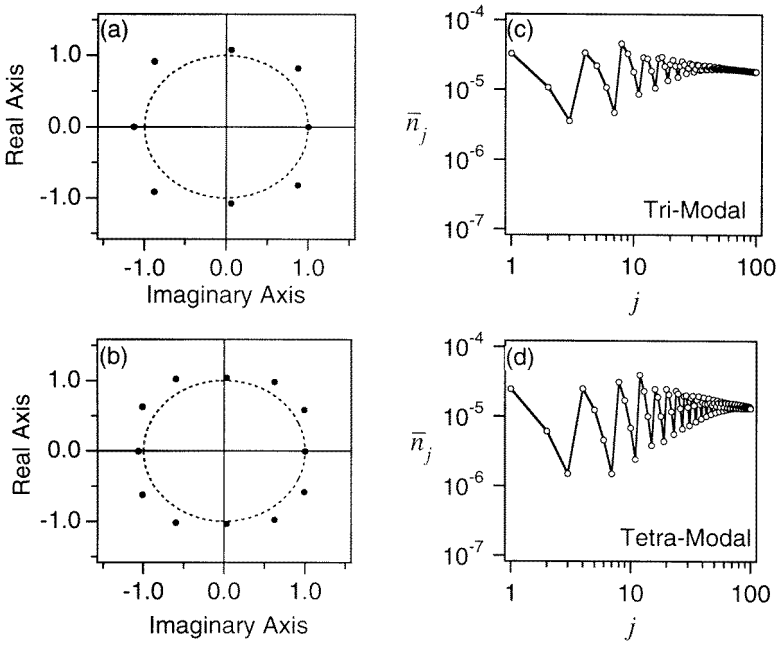

Figure 5. The roots, r_τ, of $g(z) = \frac{1}{100}$ for (*a*) a trimodal initial condition with equal number concentrations of monomers, 4-mers and 8-mers, and (*b*) tetramodal initial condition with equal number concentrations of monomers, 4-mers, 8-mers and 12-mers, respectively, plotted in the complex plane. The broken circle represents the unit circle. (*c*) Cluster-size distributions at $\tau = 100$ resulting from the trimodal, and (*d*) tetramodal initial conditions described above, respectively.

4. Similarity predictions

It is interesting to examine how the memory of initial conditions influences the scaling theory presented earlier. For the scaling relationship proposed by VDE and Friedlander (see (2)), the particle-size distributions are collapsed onto a single curve, $\psi(\eta)$, by amplifying the magnitude of n_j by $s(t)^2$, and by attenuating the magnitude of j by $1/s(t)$. Here, $s(t)$ is a measure of the average aggregate size and, as has already been mentioned, in the case of the constant kernel $s(t) \sim t$. The net effect of this scaling transform on our solution for bimodal initial conditions is illustrated in figure 6(*a*): the exponential regions of each particle-size distribution all collapse onto the curve $\psi(\eta) = \mathrm{e}^{-\eta}$ (full curve), although oscillations at small η are evident even after 100 coagulation timescales. For the choice of a constant kernel, the j value corresponding to any fixed value of $\eta = j/s(t)$ increases linearly with time. As a result, the oscillations at small j are relegated to smaller and smaller η values with increasing time. Indeed, Kreer and Penrose (1994) have shown for a constant kernel and an initial cluster-size distribution that decays at least exponentially in j, that all traces of the initial distribution are lost in the limit as $t \to \infty$ and the VDE transform of the particle-size distributions conforms exactly to $\psi(\eta) = \mathrm{e}^{-\eta}$. In this case, however, the remnants of the initial condition are only erased from $\psi(\eta)$ when $t \to \infty$ and the value of j corresponding to any fixed η is infinitely large.

What can be said about the scaling properties of the small end of the size spectrum? We found that by altering the nature of the scaling transformation it is possible to develop a

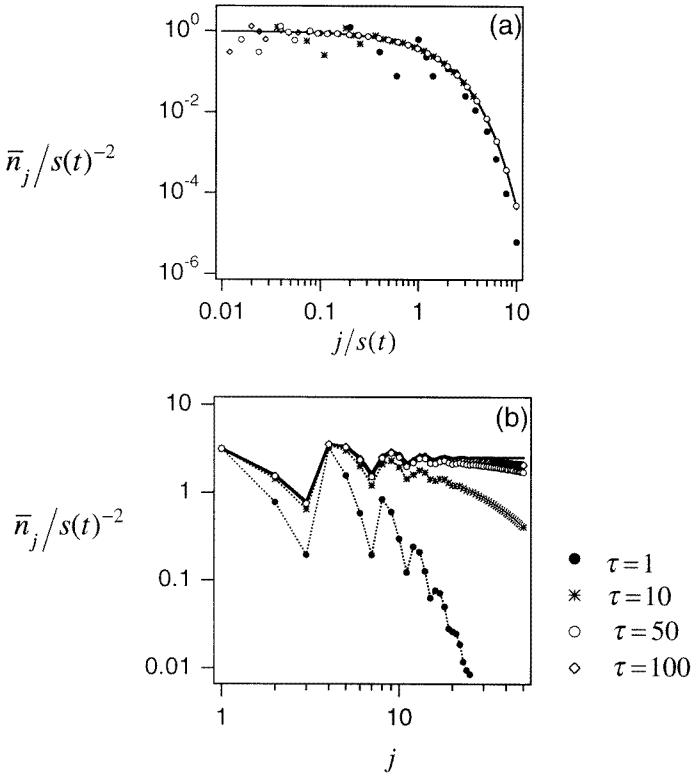

Figure 6. (*a*) Cluster-size distributions scaled according to the theory of Swift and Friedlander, and van Dongen and Ernst. The cluster-size distributions were calculated for $J = 4$ and $\alpha = \beta = 0.5$ at $\tau = 1, 10, 50$, and 100. The full curve is $\psi(\eta) = \mathrm{e}^{-\eta}$. (*b*) Cluster-size distributions scaled according to (17*a–c*) so that the small end of the size spectrum collapses onto the full curve given by $\xi(j)$.

different scaling relationship that focuses exclusively on the small end of the size spectrum. For a fixed j and in the limit as $t \to \infty$, the bimodal solution for the constant kernel exhibits the following scaling behaviour at the small end of the size spectrum:

$$n_j \sim s(t)^{-2}\xi(j) \tag{17a}$$

where

$$s(t) = \bar{N}_1/\bar{N}_\infty(\tau) \sim t \tag{17b}$$

and

$$\xi(j) = (\alpha + \beta J)^2 \sum_{l=0}^{\frac{j}{J-1}} \binom{j - l(J-1)}{l} \alpha^{j-lJ}\beta^l. \tag{17c}$$

In figure 6(*b*), we have re-plotted the same cluster distributions illustrated in figure 6(*a*) according to the relation presented in (17*a*). As illustrated in this figure, the small end of the size spectrum collapses to the curve predicted by $\xi(j)$ (full curve) within approximately 50 coagulation timescales. These results demonstrate that the memory of the initial condition is permanently etched into the small end of the size spectrum. In contrast to the VDE transformation where $\psi(\eta)$ is a universal function in the limit as $t \to \infty$, our transformation

yields a function $\xi(j)$ that depends in detail on the nature of the initial conditions (i.e. the values of α, β and J). Consequently, the shape of the small end of the size spectrum, as manifested by $\xi(j)$, is not universal.

As presented, the transformation given by (17*a–c*) is only applicable to the bimodal solution presented in this paper. However, this transformation can be generalized to include solutions of Smoluchowski's coagulation equation with a constant kernel and arbitrary initial conditions, as detailed next. Recall that the nonlinear differential equation for the generating function, $g(x,\tau) = \sum_{j=0}^{\infty} \bar{n}_j(\tau)x^j$, derived in section 2 (see (7)) is solved by changing the dependent variable to $g(x,\tau)^{-1}$. Let $g(x,\tau)^{-1} = m(x,\tau) = \sum_{j=0}^{\infty} a_j x^j$. The linearized differential equation that results for $m(x,\tau)$, $\partial/\partial\tau[m(x,\tau)] = -1$, has the solution

$$m(x,\tau) = -\tau + 1/g(x,0) \tag{18}$$

where $g(x,0)$ is the generating function that describes the initial condition. Although each $\bar{n}_j(\tau)$ evolves non-trivially with time (see (12)), the coefficients in the power series expansion for $m(x,\tau)$, a_j, evolve in a trivial fashion:

$$a_0(\tau) = -\tau - 1 \tag{19a}$$

$$a_j(\tau) = a_j(0) = -a_0(0)\sum_{i=0}^{j-1} a_i(0)\bar{n}_{j-i}(0) \qquad j \geqslant 1. \tag{19b}$$

The coefficients a_j, are computed directly from the initial distribution of clusters, $\bar{n}_j(0)$. Furthermore, for $j \geqslant 1$, a_j is a constant with respect to time, or a 'conserved quantity'. Now consider the asymptotic behaviour of $\bar{n}_j(\tau)$ as $\tau \to \infty$. It can be shown through algebraic manipulations of (8) that

$$g(x,\tau) = \frac{1}{1+\tau}\left(\frac{-1}{1-\frac{1}{1+\tau}(1+g(x,0))/g(x,0)}\right). \tag{20}$$

Expanding the fraction contained within parentheses in (20) as a truncated power series, we find

$$g(x,\tau) \sim \frac{1}{1+\tau}\left(-1-\frac{1}{1+\tau}(1+m(x,0))\right) \tag{21}$$

where $m(x,0) = 1/g(x,0) = \sum_{j=0}^{\infty} a_j(0)x^j$. Taking the limit as $t \to \infty$ of (21) gives us

$$g(x,t) \sim -\frac{1}{(1+t)^2}m(x,0) \tag{22}$$

from which we deduce the following asymptotic behaviour of $\bar{n}_j(t)$:

$$n_j \sim -\frac{1}{(1+t)^2}a_j. \tag{23}$$

Equation (23) takes on the same form as (17*a*), when it is expressed in terms of $s(t)$:

$$n_j \sim s(t)^{-2}(-\bar{N}_1^2 a_j) \tag{24}$$

and thus $\xi(j) = -\bar{N}_1^2 a_j$. Because the conserved quantities, a_j, can be specified for any initial distribution of particles, the scaling relationship given by (17*a*, *b*) applies to solutions of (1) for a constant kernel and any initial condition. The conserved quantities, a_j, presented here are closely related to the a_j described by Leyvraz (1984), although the latter only apply to kernels with $\lambda > 0$.

How might the results obtained in this study extrapolate to other frequently employed coagulation kernels (see table 1)? In general, the small end of the size spectrum is more

Table 1. Properties of common coagulation kernels. The kernels are presented assuming that the cluster stickiness, α_{ij}, is unity. The homogeneity, λ, and the small i/j limit, μ, were calculated for each physical kernel by assuming that both the hydrodynamic radius and the collision cross section radius scale with cluster size as $r_i \sim i^{1/D}$ where D is the fractal dimension of the cluster. DLA and RLA are diffusion- and rate-limited aggregation, respectively. ε is the turbulent energy dissipation rate, v is the kinematic viscosity of the fluid, T is the absolute temperature, k_b is the Boltzman constant, r_1 is the radius of a monomer, μ_v is the dynamic viscosity of the fluid, ρ_f is the density of the fluid in which coagulation takes place, $K_{1,1}$ describes the coagulation rate between two monomers, and ω is an exponent characterizing the surface area of a cluster.

Description	Kernel K_{ij}	λ	μ
	Physical kernels		
Fluid shear			
—rectilinear[a]	$\frac{1}{3}(\varepsilon/v)^{0.5}(r_i + r_j)^3$	$3/D$	0
—curvilinear[b]	$1.3(\varepsilon/v)^{0.5}(r_i + r_j)^3 E$ where $E = 1 - \frac{1+5p+2.5p^2}{(1+p)^5}$ and $p = r_i/r_j < 1$	$3/D$	0
Differential settling			
—rectilinear[c]	$\pi(r_i + r_j)^2\lvert w_i - w_j\rvert$	$1 + 1/D$	0
—curvilinear[d]	$0.5\pi(r_i^2)\lvert w_i - w_j\rvert$	$1 + 1/D$	$2/D$
Brownian diffusion (DLA)	$2k_bT/3\mu_v(1/r_i + 1/r_j)(r_i + r_j)$	0	$-1/D$
RLA	—	1	0
	Mathematical kernels		
Constant kernel	$K_{1,1}$	0	0
Product kernel	$K_{1,1}(ij)^{\omega}$	2ω	ω
Sum kernel	$K_{1,1}(i + j)/2$	1	1

[a] Saffman and Turner (1956).
[b] Landau and Lifshitz (1959).
[c] Friedlander (1977).
[d] Pruppacher and Klett (1978).

likely to retain a memory of the initial conditions when small clusters do not readily coagulate with either themselves or with larger clusters. This implies that the behaviour observed in this study for the small end of the size spectrum is most likely to occur when the coagulation kernel is characterized by λ and μ values that are greater than, or equal to, zero. This condition is not met in the case of DLA (i.e. $\mu < 0$) which may explain why Hidy (1965) found that a numerical solution of (1) with the DLA kernel and bimodal initial conditions produced self-similar cluster-size distributions consistent with (2) for $\tau > 48$. Apart from DLA, all of the physical kernels listed in table 1 are characterized by μ and $\lambda \geqslant 0$. For these kernels, the remnants of polydisperse initial conditions might very well survive for long periods of time at the small end of the size spectrum. Further research is needed to assess whether the results presented here are unique to the constant kernel, or applicable to a broader class of problems.

5. Conclusion

We have derived a solution to the discrete von Smoluchowski's coagulation equation with a constant kernel and bimodal initial conditions by use of a generating function. The resulting solution for the cluster-size distribution is described by a region of oscillation at the small end of the size spectrum, and an exponentially decaying region at the large end

of the size spectrum. We have illustrated the time evolution of the distribution and shown how the parameters describing the initial condition, namely, α, β and J, affect the cluster-size distribution through j-space. We have found that the similarity predictions made by VDE are not accessible at finite times for the small end of the size spectrum, and that fundamentally different scaling relationships describe the shapes of the small and large ends of the cluster-size spectrum.

Acknowledgments

The authors would like to thank two anonymous reviewers for their thoughtful comments on the manuscript. This work was supported by an NSF Career Award (BES-9502493) to SBG. Matching funds from the National Water Research Institute (NWRI-21851) are gratefully acknowledged.

Appendix

We being by expanding the expression for the generating function given in (11):

$$g(x,\tau) = \frac{-1+\alpha x+\beta x^J}{1+\tau} \times \frac{1}{1-\frac{\tau}{1+\tau}(\alpha x+\beta x^J)}. \tag{A1}$$

Using the definition for a geometric series, and then the binomial theorem, (A1) can be rewritten:

$$g(x,\tau) = \frac{-1+\alpha x+\beta x^J}{1+\tau} \sum_{k=0}^{\infty}\sum_{l=0}^{k}\left(\frac{\tau}{1+\tau}\right)^k \binom{k}{l} \alpha^{k-1}\beta^l x^{k+l(J-1)} \tag{A2}$$

where

$$\binom{k}{l} = \frac{k!}{(k-l)!l!}.$$

The indices of summation are changed such that $j = k + l(J-1)$. This transformation takes (A2) to

$$g(x,\tau) = \frac{-1+\alpha x+\beta x^J}{1+\tau} \sum_{j=0}^{\infty} x^j \sum_{l=0}^{\frac{j}{J-1}}\left(\frac{\tau}{1+\tau}\right)^{j-l(J-1)} \binom{j-l(J-1)}{l} \alpha^{j-lJ}\beta^l. \tag{A3}$$

We break (A3) into three sums:

$$g(x,\tau) = S_1 + S_2 + S_3 \tag{A.4a}$$

where

$$S_1 = \frac{-1}{1+\tau} \sum_{j=0}^{\infty} x^j \sum_{l=0}^{\frac{j}{J-1}}\left(\frac{\tau}{1+\tau}\right)^{j-l(J-1)} \binom{j-l(J-1)}{l} \alpha^{j-lJ}\beta^l \tag{A.4b}$$

$$S_2 = \frac{\alpha}{1+\tau} \sum_{j=0}^{\infty} x^{j+1} \sum_{l=0}^{\frac{j}{J-1}}\left(\frac{\tau}{1+\tau}\right)^{j-l(J-1)} \binom{j-l(J-1)}{l} \alpha^{j-lJ}\beta^l \tag{A.4c}$$

and,

$$S_3 = \frac{\beta}{1+\tau} \sum_{j=0}^{\infty} x^{j+J} \sum_{l=0}^{\frac{j}{J-1}}\left(\frac{\tau}{1+\tau}\right)^{j-l(J-1)} \binom{j-l(J-1)}{l} \alpha^{j-lJ}\beta^l. \tag{A.4d}$$

These three sums are treated individually. In S_1, we break off the $j = 0$ term:

$$S_1 = \frac{-1}{1+\tau} - \frac{1}{1+\tau}\sum_{j=1}^{\infty} x^j \sum_{l=0}^{\frac{j}{J-1}} \left(\frac{\tau}{1+\tau}\right)^{j-l(J-1)} \binom{j-l(J-1)}{l} \alpha^{j-lJ}\beta^l. \tag{A.5}$$

In S_2, we change the index on the outer summation from j to $j-1$:

$$S_2 = \frac{1}{1+\tau}\sum_{j=1}^{\infty} x^j \sum_{l=0}^{\frac{j-1}{J-1}} \left(\frac{\tau}{1+\tau}\right)^{j-1-l(J-1)} \binom{j-1-l(J-1)}{l} \alpha^{j-lJ}\beta^l. \tag{A.6}$$

In S_3, we change the indices used in both summations first from j to $j-J$ and then from l to $l-1$:

$$S_3 = \frac{1}{1+\tau}\sum_{j=J}^{\infty} x^j \sum_{l=1}^{\frac{j-1}{J-1}} \left(\frac{\tau}{1+\tau}\right)^{j-1-l(J-1)} \binom{j-1-l(J-1)}{l-1} \alpha^{j-lJ}\beta^l. \tag{A.7}$$

We can start the outer summation in S_3 from $j = 1$ because for j with $1 \leqslant j < J$, the upper bound of the inner summation, $(j-1)/(J-1)$, is less than 1 and so the inner summation is empty. The inner summation can be started from $l = 0$ since $\binom{n}{-1} = 0$ by convention:

$$S_3 = \frac{1}{1+\tau}\sum_{j=1}^{\infty} x^j \sum_{l=0}^{\frac{j-1}{J-1}} \left(\frac{\tau}{1+\tau}\right)^{j-1-l(J-1)} \binom{j-1-l(J-1)}{l-1} \alpha^{j-lJ}\beta^l. \tag{A.8}$$

S_2 and S_3 can be added together using the relation $\binom{n}{k-1} + \binom{n}{k} = \binom{n+1}{k}$:

$$S_2 + S_3 = \frac{1}{1+\tau}\sum_{j=1}^{\infty} x^j \sum_{l=0}^{\frac{j-1}{J-1}} \left(\frac{\tau}{1+\tau}\right)^{j-1-l(J-1)} \binom{j-l(J-1)}{l} \alpha^{j-lJ}\beta^l. \tag{A.9}$$

We would like to add (A9) to S_1, given in (A5), but the upper bound for l is $(j-1)/(J-1)$ in (A9) not $j/(J-1)$, as it is in S_1. This can only make a difference when there is an L such that $L = j/(J-1)$, $j \geqslant 1$ or $j = L(J-1)$, $L > 0$ necessarily. However, in this case, the term

$$\left(\frac{\tau}{1+\tau}\right)^{j-1-L(J-1)} \binom{j-L(J-1)}{L} \alpha^{j-LJ}\beta^L = \left(\frac{\tau}{1+\tau}\right)^{-1} \binom{0}{L} \alpha^{-L}\beta^L = 0.$$

So we may increase the upper bound to $j/(J-1)$ in (A9). Adding this to S_1, we finally obtain an expression for the generating function, $g(x, \tau)$, in increasing powers of x:

$$g(x,\tau) = -\frac{1}{1+\tau} + \frac{1}{(1+\tau)^2}\sum_{j=1}^{\infty} x^j \sum_{l=0}^{\frac{j}{J-1}} \left(\frac{\tau}{1+\tau}\right)^{j-1-l(J-1)} \binom{j-l(J-1)}{l} \alpha^{j-lJ}\beta^l. \tag{A.10}$$

Hence, by the definition of the generating function given in (6):

$$\bar{N}_\infty(\tau) = \frac{1}{1+\tau} \tag{A.11}$$

and the expression for $\bar{n}_j(\tau)$ presented in (12) is easily extracted.

References

Bak T A and Lu B 1987 *Chem. Phys.* **112** 189
Binglin L 1987 *J. Phys. A: Math. Gen.* **20** 2347
Bolle G, Cametti C, Codastefano P and Tartaglia P 1987 *Phys. Rev.* A **35** 837
Broide M L and Cohen R J 1992 *J. Colloid Interface Sci.* **153** 493
Erasmus L D, Eyre D and Everson R C 1994 *Comput. Chem. Eng.* **18** 775
Eyre D 1995 *J. Comput. Phys.* **120** 305
Fernández-Barbero A, Schmitt A, Cabrerizo-Vílchez M and Martínez-García R 1996 *Physica* A **230** 53
Friedlander S K 1977 *Smoke, Dust, and Haze* (New York: Wiley) p 194
Friedlander S K and Wang C S 1966 *J. Colloid Interface Sci.* **22** 126
Gabellini Y and Meunier J L 1992 *J. Phys. A: Math. Gen.* **25** 3683
Hidy G M 1965 *J. Colloid Interface Sci.* **20** 123
Hidy G M and Lilly D K 1965 *J. Colloid Interface Sci.* **20** 867
Jullien R 1990 *New J. Chem.* **14** 239
Jullien R, Kolb M and Botet R 1984 *Kinetics of Aggregation and Gelatin* ed F Family and D P Landau (Amsterdam: Elsevier) pp 101–9
Kobraei H R and Duncan G C 1986 *J. Colloid Interface Sci.* **113** 557
Kreer M and Penrose O 1994 *J. Stat. Phys.* **75** 389
Landau L D and Lifshitz E M 1959 *Fluid Mechanics* (New York: Pergamon) p 77
Leyvraz F 1984 *Phys. Rev.* A **29** 854
Matsoukas T and Freidlander S K 1991 *J. Colloid Interface Sci.* **146** 495
McLeod J B 1962 *Q. J. Math. Oxford* **13** 119
Meakin P 1987 *Phys. Rev.* A **35** 2234
Meakin P, Vicsek T and Family F 1985 *Phys. Rev.* B **31** 564
Melzak Z A 1953 *Q. Appl. Math.* **11** 1953
Mishra V, Kresta S M and Masliyah J H 1998 *J. Colloid Interface Sci.* **197** 57
Mulholland G W, Lee T G and Baum H R 1977 *J. Colloid Interface Sci.* **62** 406
Olivier B J, Sorensen C M and Taylor T W 1992 *Phys. Rev.* A **45** 5614
Pruppacher H R and Klett J D 1978 *Microphysics of Clouds and Precipitation* (Boston: Reidel) p 377
Saffman P G and Turner J S 1956 *J. Fluid Mech.* **1** 16
Spouge J L 1983 *J. Phys. A: Math. Gen.* **16** 3127
Swift D L and Friedlander S K 1964 *J. Colloid Interface Sci.* **19** 621
Treat R P 1990 *J. Phys. A: Math. Gen.* **23** 3003
van Dongen P G J and Ernst M H 1984 *Phys. Rev. Lett.* **54** 1396
Vicsek T and Family F 1984 *Phys. Rev. Lett.* **52** 1669
von Smoluchowski M V 1917 *Z. Phys. Chem.* **92** 129
Weitz D A, Huang J S, Lin M Y and Sung J 1984 *Phys. Rev. Lett.* **53** 1657